Oscillations in the Photoionization Cross Section of C_{60}

Y. B. Xu,[1] M. Q. Tan,[1] and U. Becker[2]
[1]*Department of Physics, Zhejiang University, Hangzhou 310027, People's Republic of China*
[2]*Fritz-Haber-Institut der Max-Planck-Gesellschaft, D-14195 Berlin, Germany*
(Received 2 January 1996)

Recent photoelectron spectroscopy results from gas phase C_{60} exhibit the same partial cross section variation with photon energy as has been observed in its solid phase. We assume that the variations originate from a fullerene specific ability to form a spherical standing wave of the final state electron by intramolecular interference or virtual reflection at the center of the photoionized molecule. The calculated photon energies of the cross section minima based on the boundary conditions of the standing wave agree fairly well with experimental data. [S0031-9007(96)00143-3]

PACS numbers: 36.40.Cg, 33.80.Eh

The study of the electronic properties of fullerenes has attracted much attention [1–4] over the years. An interesting phenomenon reported for the first time by Benning *et al.* [3] and later by Wu *et al.* [4] is the strong variation of the photoelectron line intensities of the highest occupied molecular orbital (HOMO) and HOMO-1 bands of solid phase C_{60}. Each maximum of an odd state (HOMO) is matched by a minimum in intensity of an even state (HOMO-1) as seen in Fig. 1. This phenomenon might be due to large variations in the density of states (DOS) of empty odd and even final states. To our knowledge, such large variations of the DOS extending up to 120 eV have not been observed in solid state photoemission so far.

Surprisingly, recent photoelectron spectroscopy (PES) measurements of gas phase fullerenes show very similar intensity variations [5,6] as the solid phase fullerenes. Although more measurements in smaller steps are desirable for a detailed comparison, the periodicity and the degree of variation are virtually the same. This indicates that the observed variations are not genuinely related to the DOS of solid C_{60}, and a molecular interpretation may be more appropriate. However, a calculation using molecular orbitals with alternating symmetries and free-electron-like final states also failed to describe the observed oscillations, even qualitatively [4]. In this Letter, a new explanation of the cross section variations is proposed based on the specific geometry of the fullerenes, i.e., the nearly spherical cage structure of the C_{60} molecule.

This explanation attributes the variation of the photoionization cross section to the possible formation of spherical standing waves of the final state electrons inside the molecule. An incoming spherical electron wave moving towards the center of the molecule may be virtually reflected there, producing an outgoing wave which then forms a standing wave. This effect may be considered as intramolecular interference. The amplitude of the final state wave function at the spherical shell ($r \simeq R$, where R is the radius of the skeleton of C_{60}) changes periodically with the wave number and thus with the final energy. Since the initial wave function Ψ_i of the delocalized valence electrons is distributed mainly around $r \sim R$, the photoionization matrix element $\langle \Psi_f | \hat{\mathbf{p}} | \Psi_i \rangle$ must also change periodically. This is reflected by the corresponding partial cross section. It is approximated that the potential of the electron is spherical symmetric. Therefore, the electron has a definite angular momentum (lm), and the final state wave function can be written as $\Psi_f = R_f(r) Y_{lm}(\theta, \phi)$. To begin our examination of the partial cross section modulation, we assume an extremely simple potential $U(r)$ which equals a constant $(-U_m)$ inside the molecule (or inside the solid) and vanishes outside. As a result, the radial wave function inside has the form of a spherical Bessel function

$$R_f \sim j_l(k_m r), \tag{1}$$

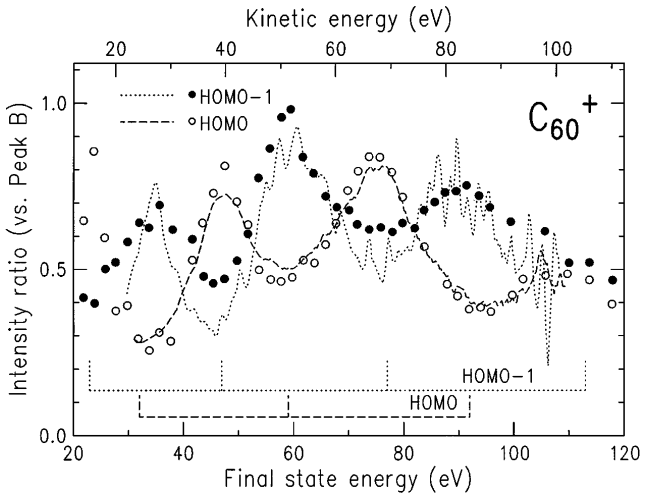

FIG. 1. Photoemission intensity variations as a function of final state energy ($E_f = E + \mathrm{IP}_{\mathrm{HOMO}}$) with respect to the HOMO level. The intensities from solid C_{60} from Ref. [3] (open and filled circles) are normalized to that of peak B (peak 4) which originates from a mixture of odd and even states [8]. The data from Ref. [4] (dashed and dotted line) have been normalized to the relative intensities of Ref. [6] before the ratio with respect to peak B was taken. The bar diagram indicates the minima positions in the partial cross sections (model A).

 0031-9007/96/76(19)/3538(4)$10.00

where $k_m = \frac{1}{\hbar}\sqrt{2m(E + U_m)}$ and E is the electron's kinetic energy, or, in other words, the final electron energy with reference to the vacuum level. The energy E at the PES intensity minima is given by $j_l(k_m R) = 0$ in both the gas and the condensed phase. Taking the final state angular momentum $l_f = 4$ (from HOMO) or 3 (from HOMO-1) (discussed further later), the final energies at the intensity minima are easily calculated using the above equation. The only free parameter in the above formula is the potential U_m, because R is known to be 3.54 Å. The best fit from the experimental data yields a value for $U_m = 17.5$ eV. The final energies (with reference to the initial HOMO level $E_f = E + 7.61$ eV) calculated semiempirically are shown by the bars in Fig. 1 and are listed in the first column of Table I. (Note that only the final energies within the range 20–100 eV are listed). The experimental sequence of minima given in the third column agrees quite well with the calculation, particularly considering the simple approximation used for the potential.

The choice of l_f is based on the selection rule $l_f = l_i \pm 1$. The angular quantum number of the initial HOMO-1 states ($G_g + H_g$) is $l_i = 4$ [7,8], and that of the HOMO states (H_u) is $l_i = 5$. For very large l_f, the amplitude of the final wave function at $r \approx R$ should always be small due to the high centrifugal barrier. (The wave function is normalized mainly for large r.) Such final states will not contribute significantly to the photoelectron spectra. Hence, as a rough approximation, we take the least possible l_f, i.e., $l_f = 4$ (excited from HOMO) and $l_f = 3$ (excited from HOMO-1), respectively.

This simple potential, however, is probably not very realistic, and the perceived agreement with the experimental data could be fortuitous because it does not account specifically for the fact that the initial state is distributed around $r = R$. In order to correct for this distribution, a potential, which is more realistically experienced by the photoelectron, is introduced in the following way (model B).

(1) The potential energy U of the final electron in the C_{60} molecule is still spherical symmetric so that the final electron has a definite angular momentum. The radial variation of $U(r)$ is depicted in Fig. 2(a).

TABLE I. Final state energies (eV).

Valence orbital	Model A	Model B	Experiment [3]
HOMO	32	31	34
	59	59	58
	92	93	93
HOMO-1	23	23	23
	47	47	46
	77	78	76

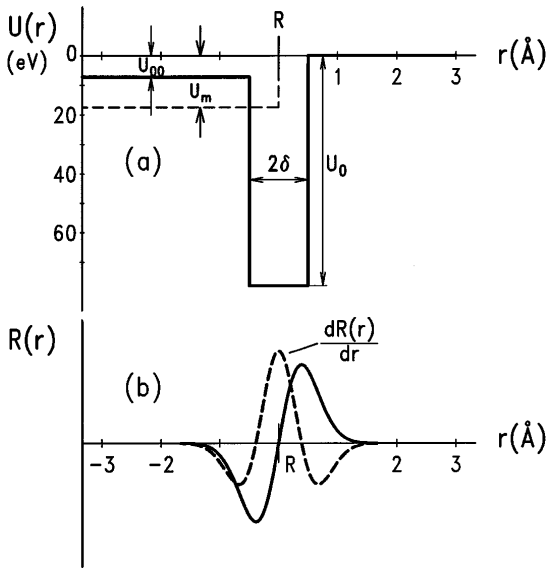

FIG. 2. (a) Simplified potential energy of the final state electron as a function of r for cases A and B (dotted and solid lines). (b) Schematic representation of the symmetry of radial wave function $R_i(r)$ of the initial HOMO and HOMO-1 states along with its derivative.

(2) The centrifugal potential changes rapidly only inside the hollow molecule ($r < R - \delta$) and can be approximated as a constant within the shell ($R - \delta < r < R + \delta$) and as zero outside the shell ($r > R + \delta$).

Using this model the radial part of the final state wave function takes the following different forms in the three regions: for $r < R - \delta$,

$$R_f(r) = A j_l(k_0 r);$$

for $R - \delta < r < R + \delta$,

$$R_f(r) = \frac{B}{k' r} \sin\left(k' r - \frac{l}{2}\pi + \delta_l'\right);$$

for $r > R + \delta$,

$$R_f(r) = \frac{1}{kr} \sin\left(kr - \frac{l}{2}\pi + \delta_l\right); \qquad (2)$$

where j_l is the spherical Bessel function of order l, and k_0, k', and k are given by

$$\frac{\hbar^2 k_0^2}{2m} = E + U_{00},$$

$$\frac{\hbar^2 k'^2}{2m} = E + U_0 - \frac{\hbar^2 l(l+1)}{2mR^2},$$

$$\frac{\hbar^2 k^2}{2m} = E.$$

E is the final energy, and δ_l is the phase shift. The amplitude in the region $r > R + \delta$ has been suitably

normalized. The boundary conditions between adjacent regions lead to the following equations:

$$A_{j_l}(k_0R - k_0\delta) = \frac{B}{k'(R-\delta)} \times \sin\left(k'R - k'\delta - \frac{l}{2}\pi + \delta_l'\right), \quad (3)$$

$$\frac{j_l(k_0R - k_0\delta) + k_0(R-\delta)j_l'(k_0R - k_0\delta)}{(R-\delta)j_l(k_0R - k_0\delta)} = k'\cot\left(k'R - k'\delta - \frac{l}{2}\pi + \delta_l'\right), \quad (4)$$

$$kB\sin\left[k'(R+\delta) - \frac{l}{2}\pi + \delta_l'\right] = k'\sin\left[k(R+\delta) - \frac{l}{2}\pi + \delta_l\right], \quad (5)$$

$$k'\cot\left[k'(R+\delta) - \frac{l}{2}\pi + \delta_l'\right] = k\cot\left[k(R+\delta) - \frac{l}{2}\pi + \delta_l\right], \quad (6)$$

where $j_l'(x)$ is the derivative of $j_l(x)$ with respect to x. From these equations, A, B, δ_l, and δ_l' can be solved as functions of k or E, and Ψ_f can be determined.

First, we are interested in the periodicity of the cross section variation. The simplest thing we can do is to determine the final energies at the cross section minima, which corresponds to $\langle\Psi_f|\hat{\mathbf{p}}|\Psi_i\rangle = 0$. Here we argue more rigorously the condition of $R_f(R)$ for the intensity minima. Consider the Hermitian conjugate matrix element $\langle\Psi_i|\hat{p}_x|\Psi_f\rangle^* = 0$ with $\hat{p}_x = -i\hbar\frac{\partial}{\partial x} = -i\hbar(Y_{1,1} + Y_{1,-1})\frac{\partial}{\partial r}$ + angular derivatives. It can be argued that when $k'R \gg l$ the radial derivative dominates. In the energy range of interest, $k'R$ amounts to 20–30. Under this condition the intensity minimum occurs approximately when $\int_0^\infty R_f^*(r)\frac{\partial}{\partial r}R_i(r)r^2\,dr \simeq 0$. For the HOMO and HOMO-1 states, the initial wave functions are derived from π bonds [3]. So the radial part $R_i(r)$ is antisymmetric about the point $r = R$, and $\frac{d}{d_r}R_i(r)$ is symmetric [see Fig. 2(b)]. Thus, if the final state radial wave function in the region $(R - \delta < r < R + \delta)$ satisfies $R_f(R) = 0$, i.e. [see Eq. (2)],

$$k'R - \frac{l}{2}\pi + \delta_l' = n\pi, n = 0, 1, 2, \ldots, \quad (7)$$

the cross section will give approximately a minimum. Substituting Eq. (7) into Eq. (4), we get

$$k_0(R-\delta)j_l'(k_0R - k_0\delta) + [1 + k'(R-\delta)\cot k'\delta] \times j_l(k_0R - k_0\delta) = 0. \quad (8)$$

The values of k or E giving the minimum cross sections can be solved from Eq. (8).

Although the above formulas were derived for the gas phase (a single C_{60} molecule), they also apply for the solid. Since the energy range of interest is 25–120 eV (above E_F), the mean free path without inelastic scattering amounts to $\sim$1 nm. The waves which are elastically scattered by other C_{60} molecules are attenuated by both the r^{-2} law and the inelastic scattering, and can either be neglected at the spherical shell of the photoionized molecule or make relatively featureless contributions to the cross section. Note that the electron potential energy in the region $r > R + \delta$ should be changed from Fig. 2(a). But this does not influence Eq. (8), and thus the variation of cross section has the same period for both the gas phase and solid phase. To solve Eq. (8) one has to assign the potential parameters. Based on the muffin-tin potential used for carbon solids [9], the average half thickness of the deep potential shell containing the carbon atoms is estimated to be about $\delta = 0.5$ Å, and the shallow potential in the hollow space to be $-U_{00} = -7.2$ eV. The remaining deep potential parameter U_0 is then adjusted to give a best fit to the six final state experimental energies at the photoemission cross section minima. The physical meaning of this parameter should not be overemphasized; in our description it plays basically the role of an adjustable parameter. For $U_0 = 78$ eV (near best fit in our simple square potential model), the numerical values of the final state energies (with reference to the HOMO level) for the cross section minima are listed in the second column

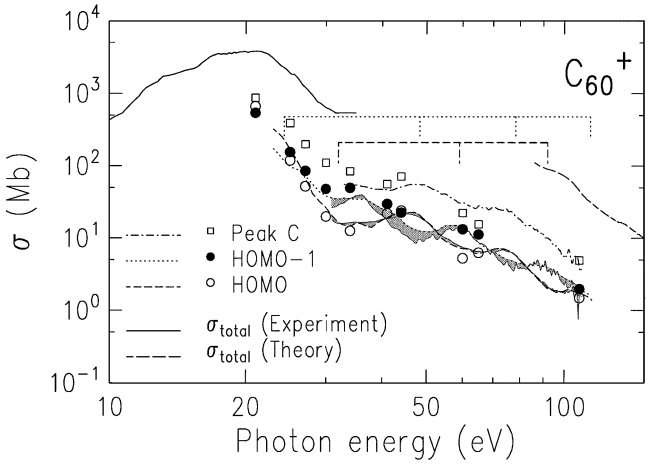

FIG. 3. Partial cross sections of the three outermost levels of molecular (open and filled circles, and open squares [5,6]) and solid (dashed [3], dotted [3], dash-dotted [4], and thin solid lines [4]) C_{60} as a function of photon energy along with the bar diagram for the minima positions of the partial cross section modulations (model A). Note that maxima and minima do not match in the presentation because of the binding energy difference of the two orbitals (1.28 eV). The total cross section used for calibration is derived from experimental data [10,11] and theoretical extrapolations [12,13], the absolute scale being based on thin film measurements [14] as an upper limit.

of Table I. They are also displayed in Fig. 3, which shows the corresponding partial cross sections of the three outermost orbitals for both gas phase [5,6] and solid [3,4] on a logarithmic scale versus photon energy.

The alternating cross section modulations are also exhibited by other valence photolines (see the five topmost curves in Fig. 7 of Ref. [4]) but less and less pronounced with increasing binding energy. They finally disappear for core level photoemission because of the increasing localization of the corresponding electron density distribution.

Model B, despite being quite simple, is a more realistic one than model A, yet agrees equally well with the experimental results of Benning *et al.* [3] and Wu *et al.* [4]. Also, the potential parameters used in model B have reasonable values compared to the muffin-tin potential for carbon solids [9]. This seems to indicate that our conclusion regarding the origin of the variation of the photoemission partial cross section is, in principle, correct. This result does not depend on the particular shape of the chosen potential, which may, however, have some effect on the potential depths.

The variation is determined by the geometry of the molecule, or, more specifically, the changing overlap of the standing spherical wave of the final state electron with the initial state wave function, rather than by the electron DOS at the final state energy. The mechanism of this variation is indirectly related to that of extended x-ray-absorption fine structure (EXAFS), or, more specifically, to valence photoelectron diffraction. One could call this phenomenon "partial cross section fine structure due to intramolecular interference" or "initial state induced photoelectron diffraction pattern."

This phenomenon is closely linked to quantum well phenomena [15], in particular, quantum well resonance [16], because the standing waves can be considered as eigenstates of a three-dimensional quantum sphere, which are quenched in photoemission due to the vanishing overlap with the spherically distributed initial state. Assuming the discussed fullerene specific explanation is true, the described behavior should also be exhibited by other fullerenes. This can easily be tested by conducting further measurements. First results from C_{70} [17], solid C_{86}, and solid C_{90} [18] point to this direction.

In conclusion, we have shown that unusual variations in the partial photoionization cross section of the outermost valence orbitals of solid and gaseous C_{60} can be explained by a simple model based on the geometric structure of this molecule, employing the formation of standing waves. However, more detailed and quantitative partial cross section calculations by, e.g., the multiple scattering approach, the atomic central field approximation, or molecular orbital theory, along with corresponding measurements, are needed to validate this model.

This work was sponsored by the Bundesministerium für Bildung, Wissenschaft, Forschung und Technologie (BMBF) and by the Deutsche Forschungsgemeinschaft (DFG). One of the authors (Y.B.X.) is indebted to the Humboldt Foundation and the China Natural Science Foundation for financial support.

[1] J. H. Weaver, J. L. Martins, T. Komeda, Y. Chen, T. R. Ohno, G. H. Kroll, N. Troullier, R. E. Haufler, and R. E. Smalley, Phys. Rev. Lett. **66**, 1741 (1991).

[2] J. H. Weaver and D. M. Poirer, in *Solid State Physics*, edited by H. Ehrenreich and F. Spaepen (Academic Press, New York, 1994), Vol. 48.

[3] P. J. Benning, D. M. Poirier, N. Troullier, J. L. Martins, J. H. Weaver, R. E. Haufler, L. P. Chibante, and R. E. Smalley, Phys. Rev. B **44**, 1962 (1991).

[4] J. Wu, Z. Shen, D. Dessau, R. Cao, D. Marshall, P. Pianetta, I. Lindau, X. Yang, J. Terry, D. King, B. Wells, D. Elloway, H. Wendt, C. Brown, H. Hunziker, and M. de Vries, Physica (Amsterdam) **197C**, 251 (1992).

[5] D. Lichtenberger, M. Jatcko, K. Nebesny, C. Ray, D. Huffman, and L. Lamb, in *Clusters and Cluster-Assembled Materials*, edited by R. Averback, D. Nelson, and J. Bernholc (MRS, Pittsburgh, 1991), p. 673.

[6] T. Liebsch, O. Plotzke, F. Heiser, U. Hergenhahn, O. Hemmers, R. Wehlitz, J. Viefhaus, B. Langer, S. B. Whitfield, and U. Becker, Phys. Rev. A **52**, 457 (1995).

[7] R. C. Haddon, L. E. Brus, and K. Raghavachari, Chem. Phys. Lett. **125**, 459 (1986).

[8] J. L. Martins, N. Troullier, and J. H. Weaver, Chem. Phys. Lett. **180**, 457 (1991).

[9] Y. Zhou and J. C. Tang, J. Phys. Condens. Matter **6**, 2949 (1994); (private communication).

[10] A. Ding, in *Electron Collisions with Molecules, Clusters, and Surfaces*, edited by H. Ehrhardt and L. Morgan (Plenum, New York, 1994).

[11] I. Hertel, H. Steger, J. de Vries, B. Weisser, C. Menzel, B. Kamke, and W. Kamke, Phys. Rev. Lett. **68**, 784 (1992).

[12] G. Wendin and B. Wästberg, Phys. Rev. B **48**, 14 764 (1993).

[13] J. Yeh, *Atomic Calculation of Photoionization Cross Sections and Asymmetry Parameters* (Gordon and Breach, Langhorne, 1993).

[14] S. Ren, Y. Wang, A. Rao, E. McRae, J. Holden, T. Hager, K. Wang, W. Lee, H. Ni, J. Selegue, and P. Eklund, Appl. Phys. Lett. **59**, 2678 (1991).

[15] M. F. Crommie, C. P. Lutz, and D. M. Eigler, Science **262**, 218 (1993).

[16] T. Miller, A. Samsavar, and T. Chiang, Phys. Rev. B **50**, 17 686 (1994).

[17] T. Liebsch, O. Plotzke, R. Hentges, A. Hempelmann, U. Hergenhahn, F. Heiser, J. Viefhaus, U. Becker, and Y. Xu (to be published).

[18] S. Hino, K. Umishita, K. Iwasaki, T. Miyazaki, K. Kikuchi, and Y. Achiba, Phys. Rev. B **53**, 7496 (1996).